2023 IEEE/RSJ International Conference on Intelligent Robots and Systems (IROS)
October 1-5, 2023. Detroit, USA

Incorporating Stochastic Human Driving States in Cooperative Driving Between a Human-Driven Vehicle and an Autonomous Vehicle

Sanzida Hossain[1], Jiaxing Lu[2], He Bai[1] and Weihua Sheng[2]

Abstract— **Modeling a human-driven vehicle is a difficult subject since human drivers have a variety of stochastic behavioral components that influence their driving styles. We develop a cooperative driving framework to incorporate different human behavior aspects, including the attentiveness of a driver and the tendency of the driver following advising commands. To demonstrate the framework, we consider the merging coordination between a human-driven vehicle and an autonomous vehicle (AV) in a connected environment. We propose a stochastic model predictive controller (sMPC) to address the stochasticity in human driving behavior and design coordinated merging actions to optimize the AV input and influence human driving behavior through advising commands. Simulation and human-in-the-loop (HITL) experimental results show that our formulation is capable of accommodating a distracted driver and optimizing AV inputs based on human driving behavior recognition.**

I. INTRODUCTION

Autonomous vehicles (AVs) are entering the transportation systems at an increasing pace. It is estimated that more than 33 million AVs will be sold worldwide in 2040, with 7.4 million of those being sold in the United States, 14.5 million in China, 5.5 million in European countries, and 6.3 million in other international markets [1]. It is expected that AVs and human-driven vehicles will co-exist for a long time. Therefore, it is important to consider how to ensure safety in mixed traffic consisting of both AVs and human-driven vehicles. Cooperative driving between AVs and human-driven vehicles is a way to improve transportation safety in mixed traffic scenarios.

To facilitate cooperative driving, appropriate human modeling of stochastic elements in human behaviors is crucial. Researchers have worked on human driver modeling for applications in driver assistance systems in the last decade. In [2], the authors use hidden mode stochastic hybrid systems to simulate the interaction between the driver and the vehicle in an assistive driving system. In [3], partially observable Markov decision processes (POMDPs) are used to develop a unified framework modeling machine dynamics and human behavior in HITL control of semi-autonomous vehicles.

Cooperative driving in mixed traffic has been attracting great interest from many researchers in recent years. The authors in [4] establish risk-bounded motion policies using a chance-constrained POMDP for AVs when the system is uncertain due to human intervention or road conditions. In [5], future environmental data are predicted, and the optimal action for the AV is adjusted to account for anticipated changes in future prediction. Reference [6] investigates the control of connected AVs to react properly to uncertain maneuvers of human-driven vehicles. Reference [7] considers how AVs can influence the behavior of human-driven vehicles. The aforementioned references focus on human-AV interaction and predict or influence human driving behavior to optimize AV maneuvers. However, human-driven vehicles are considered disconnected to the AVs and can only be indirectly influenced. They do not consider AVs operating with human-driven vehicles in a connected environment.

In this paper, we investigate cooperative driving between AVs and human-driven vehicles in a connected environment for a lane merging scenario. We consider an intelligent human-driven vehicle (IHV) that can monitor driver status, provide advisory commands, sense its environment, and exchange information with surrounding connected vehicles through vehicle-to-vehicle (v2v) communication. We propose a discrete system for IHV and AV interaction, using stochastic model predictive control (sMPC) to generate control inputs and advisory commands. In [8], [9], [10], we formulate the optimization of cooperative driving between an IHV and an AV considering only one driver's state, i.e., the driver's tendency to follow advisory commands. Building on [8], [10], we develop a multi-state cooperative driving framework to incorporate human driver's attentiveness as an additional state, since human drivers behave differently when driving inattentively. The framework can be extended to accommodate any number of human states.

The rest of this paper is organized as follows. The driver's state understanding including distraction detection and human maneuver modeling is presented in Section II. The hybrid system modeling for the coordination of AV and IHV is presented in Section III. The system constraints and the sMPC formulation are discussed in Section IV and V, respectively. Simulation results for the proposed sMPC are presented in Section VI. HITL experimental results validating the performance of our method are given in Section VII. Conclusions and future work are discussed in Section VIII.

II. DRIVER STATE UNDERSTANDING

An AV can be effectively controlled to complete a complex driving task efficiently. On the other hand, a human driver, depending on her/his skill of driving and attention state, may struggle to perform the same task without guidance

[1]Sanzida Hossain and He Bai are with Mechanical and Aerospace Engineering, Oklahoma State University, Stillwater, OK 74078, USA. {sanzida.hossain, he.bai}@okstate.edu

[2]Jiaxing Lu and Weihua Sheng are with Electrical and Computer Engineering, Oklahoma State University, Stillwater, OK 74078, USA. {jiaxing.lu,weihua.sheng}@okstate.edu

This work is supported by the National Science Foundation (NSF) Grants CISE/IIS 1910933 and CPS 2212582.

2023 IEEE/RSJ International Conference on Intelligent Robots and Systems (IROS) | 978-1-6654-9190-7/23/$31.00 ©2023 IEEE | DOI: 10.1109/IROS55552.2023.10341565

or advice. Unlike robotic drivers in AVs, human drivers possess characteristics such as uncertainty and flexibility. Understanding human's state of driving is critical for developing a cooperative driving system for a mixed traffic scenario.

We consider two characteristics of human driving behavior to formulate the human driver model: first, whether the human is following an announced advisory command, and second, whether the human is attentive or distracted. We denote by x_k^B the binary state of whether the human driver is following the advisory, where the subscript $k \in \mathbb{Z}_+$ is the discrete-time index. $x_k^B = 1$ means that the human is following the advisory command. Otherwise, $x_k^B = 0$. We also define the binary state $a_k = \{0,1\}$ as the driver's attention state. If the driver is attentive, $a_k = 1$, otherwise $a_k = 0$.

We propose two distinct models for detecting and comprehending human driver's behavior in the cooperative driving system. The first model focuses on detecting the human driver's distraction using image data from a camera observing the driver, while the second model is capable of recognizing the maneuver actions of the human driver and thus inferring the driver's tendency to follow, based on vehicle control data such as gas pedal, brake, etc.

A. Distraction detection

Distraction detection is an important task in the field of assisted driving. To detect instances of distracted driving using camera data, we trained a Residual Network (ResNet-50). The proposed model is a deep neural network that consists of 50 layers, allowing it to extract high-level features from video frames. The image classification algorithm categorized 7 types of distracted driving behaviors and 1 type of normal driving behavior given in Table I.

TABLE I

CATEGORIES OF HUMAN DRIVING BEHAVIOR

safe driving	drinking/eating
texting on the phone	reaching behind
talking on the phone using the left hand	talking to the passenger
talking on the phone using the right hand	doing hair and makeup

We fine-tuned the pre-trained ResNet-50 model on a mixed dataset of local samples collected in our laboratory and images from an open-source database. The architecture of the ResNet-50 model can be found in [11]. The input images were resized to $224 * 224$ pixels and then trained on a powerful computer. The resulting merged dataset improved the accuracy of our model to 95% during testing, making it adaptable to both laboratory and real-world driving scenarios.

During inference, we utilized a Jetson Nano and a camera to capture the driver's top half image at 5hz frequency. The model resized the image and then processed it to generate a probability matrix of 8 classes. By extracting the probability value for normally driving from the matrix, we derived the probability of attentive driving $P(a_k = 1)$.

B. Human driver maneuver modeling

In a cooperative driving HITL system that interacts with the human driver by providing guidance and advice, it is important to assess the effectiveness of the advice, in other words, the driver's tendency of following. To determine the driver's tendency of following, we need to recognize the driving action of the human driver and then compare it with the advice. To achieve this, we employed an HMM-based probability model, which was previously introduced in [10].

We defined an action set of the human driver as, $\mathbf{A} = \{accelerate, decelerate, maintain\}$, which includes events of speeding up, slowing down, and maintaining a constant speed, respectively. We trained an HMM model for each action, using the driving data that includes gas pedal percentage, brake pedal percentage, and vehicle velocity. During inference, a sequence of driving data is fed into each of these models, and a probability distribution is obtained, which represents the probability of the sequence fitting each HMM model. Comparing it with the advised action from the previous guidance for the human driver, the probability of tendency of following, $P(x_k^B = 1)$, is obtained.

III. DYNAMIC MODELS OF AV AND IHV

We consider the coordination of lane merging between an AV and an IHV as shown in Fig. 1. The goal is to quickly create the gap between the cars for a secure and seamless merging. The AV can be directly controlled through control inputs but only the driver can have an impact on the motion of the IHV. The driver's action can be influenced through advisory directives. To identify the optimal advisory instructions for the IHV and the best autonomous controls for the AV, we propose an sMPC problem with constraints on both state and control. In this section, we discuss the dynamic models used in the sMPC. Sections IV and V present the constraints and the sMPC formulation, respectively.

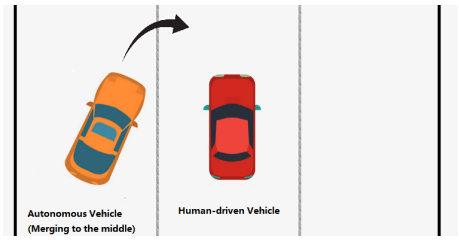

Fig. 1. Merging scenario considered in this paper.

A. AV dynamics

We consider a linear dynamic model of an AV

$$x_{k+1}^r = A_r x_k^r + B_r u_k^r, \tag{1}$$

where the longitudinal position and velocity with respect to the origin are represented by $x_k^r \in \mathbb{R}^2$, A_r and B_r are matrices of suitable dimensions that define the AV dynamics, and $u^r \in \mathbb{R}$ is the input (acceleration) to the AV.

B. IHV dynamics

The IHV dynamics is modeled as discrete hybrid stochastic automata (DHSA) [12]. We model the human driver's states as discrete parameters. The IHV dynamics can change between different models based on these discrete states.

We denote the set of possible human states by one hot encoded vector $S_k = [s_k^1, s_k^2, \ldots, s_k^n]^\top \in \mathbb{Z}^n$ where $s_k^1, s_k^2, \ldots, s_k^n \in \{0,1\}$, each representing a discrete human state and n is the total number of possible states. Only one element in S_k is 1 while all other elements are zero. Each non-zero s_k^i, where $i \in \{1, \cdots, n\}$, represents a different combination of behavioral aspects being considered. Specifically, we consider two aspects of human driver behavior: the following state x_k^B and the attention state a_k. Based on x_k^B and a_k, there are in total four human states: 1) distracted and not following, 2) distracted and following, 3) attentive and not following, and 4) attentive and following. When in a distracted state, humans tend to behave similarly regardless of whether they follow instructions or not. Due to this reason, we consider the following three states $S_k = [s_k^1, s_k^2, s_k^3]$ defined as

$$s_k^1 = 1 \Leftrightarrow a_k = 0,\ x_k^B = 0 \text{ or } 1, \tag{2}$$
$$s_k^2 = 1 \Leftrightarrow a_k = 1,\ x_k^B = 0, \tag{3}$$
$$s_k^3 = 1 \Leftrightarrow a_k = 1,\ x_k^B = 1. \tag{4}$$

Depending on the current human state, the dynamics of the IHV is given by

$$s_k^1 = 1 \Rightarrow x_{k+1}^h = A_h x_k^h + B_h u_k^d, \quad s_{k+1}^a = u_k^d, \tag{5}$$
$$s_k^2 = 1 \Rightarrow x_{k+1}^h = A_h x_k^h + B_h u_k^h, \quad s_{k+1}^a = u_k^h, \tag{6}$$
$$s_k^3 = 1 \Rightarrow x_{k+1}^h = A_h x_k^h + B_h s_k^a, \quad s_{k+1}^a = \lambda s_k^a + (1-\lambda) u_k^a, \tag{7}$$

where A_h and B_h are matrices of suitable dimensions that define the IHV dynamics, $u_k^d \in \mathbb{R}$ is the human input when the human is distracted (inattentive), $u_k^h \in \mathbb{R}$ is the human input when the human is not distracted, $u_k^a \in \mathbb{R}$ is the advisory commands for the IHV. The human inputs u_k^d and u_k^h can be predicted using the method presented in [10].

In (7) where $s_k^3 = 1$, the human tries to follow a given advisory control. As the human driver tries to execute an advisory command, there is a delay. As a result, rather than being applied instantly to the vehicle, the advising directive is gradually executed by the human driver. More delays can result from the computation lag of the optimal commands and the transmission and announcement delay of the advised commands. To take these delay effects into account, we employ a first-order system of the form shown in (7). The state s_k^a holds the input applied from the previous step to account for that delay. The reaction constant $\lambda \in [0,1)$ represents how fast the human in the IHV is adapting to the advisory action u_k^a after it is announced. If $\lambda = 0$, the driver applies the advised control command u_k^a exactly at the $(k+1)^{th}$ step. In other words, it is anticipated that the calculation, announcement, and driver tracking of the advisory directives will all be finished in a single step. As $\lambda \to 1$, the driver's response to the advisory action u_k^a is slowed down. Note that the first-order delay model can be replaced by other human actuation dynamics, such as the second-order dynamics in [13], [14].

Define $\bar{x}_k^h = [x_k^h; s_k^a]$. We rewrite the dynamics (5)–(7) as

$$\bar{x}_{k+1}^h = \begin{bmatrix} A_h & 0 \\ 0 & 0 \end{bmatrix} \bar{x}_k^h + \begin{bmatrix} B_h & B_h & B_h & 0 \\ 1 & \lambda & 1 & (1-\lambda) \end{bmatrix} \begin{bmatrix} \bar{z}_k^1 \\ \bar{z}_k^2 \\ \bar{z}_k^3 \\ \bar{z}_k^4 \end{bmatrix}, \tag{8}$$

where $\bar{z}_k^1 = s_k^1 u_k^d$, $\bar{z}_k^2 = s_k^3 s_k^a$, $\bar{z}_k^3 = s_k^2 u_k^h$, and $\bar{z}_k^4 = s_k^3 u_k^a$. Based on $\bar{z}_k^1$, $\bar{z}_k^2$, $\bar{z}_k^3$, $\bar{z}_k^4$, and the initial conditions x_0^r and x_0^h, we obtain the solution to x_k^h and s_k^a as:

$$x_k^h = A_h^k x_0^h + \sum_{j=0}^{k-1} A_h^{k-j-1} B_h \left(\bar{z}_j^1 + \bar{z}_j^2 + \bar{z}_j^3\right), \tag{9}$$
$$s_{k+1}^a = \bar{z}_k^1 + \lambda \bar{z}_k^2 + \bar{z}_k^3 + (1-\lambda)\bar{z}_k^4. \tag{10}$$

C. Stochastic human state transitions

We consider human state transitions from s_k^i to s_{k+1}^j as stochastic events and define one hot encoded $t_k = [t_k^1, t_k^2, \ldots, t_k^{n^2}]$, where n is the number of discrete human states and each element $t_k^p \in \{0,1\},\ \forall\ p \in \{1,2,\ldots,n^2\}$, indicates an event of transitioning from $s_k^i = 1 \to\ s_{k+1}^j = 1$ when $u_k^B = 1$ (advising on) where $i, j \in \{1,2,\ldots,n\}$. Similarly, we define one hot encoded $\bar{t}_k = [\bar{t}_k^1, \bar{t}_k^2, \ldots, \bar{t}_k^{n^2}]$, where each element $\bar{t}_k^p \in \{0,1\},\ \forall\ p \in \{1,2,\ldots,n^2\}$, indicates an event of transitioning from $s_k^i = 1 \to s_{k+1}^j = 1$ when $u_k^B = 0$ (advising off) where $i, j \in \{1,2,\ldots,n\}$.

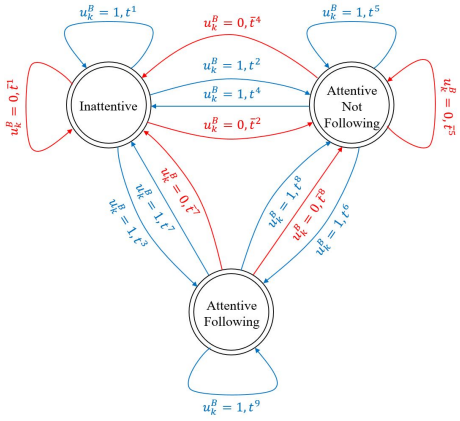

Fig. 2. sFSM for human state transitions. Blue transitions indicate transitions for $u_k^B = 1$ and red transitions indicate the transitions for $u_k^B = 0$.

The transitions in our system where $n = 3$ is illustrated using a stochastic finite state machine (sFSM) in Fig. 2. The total number of possible transitions is 18. Among these transitions, the transitions that are not possible to occur have probabilities of 0. These transitions are not shown in the sFSM. In total, we have 15 transitions.

IV. System Constraints

We take into account the following four sets of constraints to coordinate the actions of the IHV and the AV.

A. State constraints:

The new variables $\bar{z}_k^1, \bar{z}_k^2, \bar{z}_k^3$ and $\bar{z}_k^4$ and their relationships with the states and inputs lead to state constraints. The state and input limits are also included in these constraints. Using the mixed-logic dynamical (MLD) systems formulation in [15], the state constraints are formulated as inequalities. The expressions of these inequalities can be found in [11].

B. Human state transition constraints:

Following the human state transition from the sFSM, each transition from s_k^i to s_{k+1}^j for $u_k^B = 1$ is encoded by the binary event t_k^p. Therefore, the event t_k^p takes place only when $s_k^i = s_{k+1}^j = u_k^B = 1$. Such a transition is converted to the following inequality constraints:

$$s_{k+1}^j + s_k^i + u_k^B \leq 2 + t_k^p,\ t_k^p \leq s_k^i,\ t_k^p \leq s_{k+1}^j,\ t_k^p \leq u_k^B. \quad (11)$$

Similarly, each transition from s_k^i to s_{k+1}^j when $u_k^B = 0$ is encoded by the binary event $\bar{t}_k^p$ and the event $\bar{t}_k^p$ takes place only when $s_k^i = s_{k+1}^j = (1 - u_k^B) = 1$. This transition is formulated using the following inequalities:

$$s_{k+1}^j + s_k^i - u_k^B \leq 1 + \bar{t}_k^p,\ \bar{t}_k^p \leq s_k^i,\ \bar{t}_k^p \leq s_{k+1}^j,\ \bar{t}_k^p \leq (1 - u_k^B). \quad (12)$$

Each event pair $\{t_k^p, \bar{t}_k^p\},\ \forall p \in \{1, 2, \ldots, 3^2\}$ will produce constraints similar to (11)–(12). Since only one event occurs in the k^{th} time step, it follows that

$$t_k^1 + t_k^2 + \cdots + t_k^{n^2} + \bar{t}_k^1 + \bar{t}_k^2 + \cdots + \bar{t}_k^{n^2} = 1. \quad (13)$$

The transition probability of an event t_k^p is denoted by $P(t_k^p) = P(s_{k+1}^j = 1 | s_k^i = 1, u_k^B = 1)$. Similarly the transition probability of an event $\bar{t}_k^p$ is denoted by $P(\bar{t}_k^p) = P(s_{k+1}^j = 1 | s_k^i = 1, u_k^B = 0)$. These transition probabilities indicate the human's driving pattern and level of compliance, which can be estimated based on prior driving data. For simulation and experiments in this paper, we have carefully chosen the transition probabilities, which can be found in [11].

In the initial step $k = 0$, the probabilities $P(x_0^B = 1)$ and $P(a_0 = 1)$ are estimated as described in Section II. We assume that the two estimated probabilities are independent, resulting in $P(s_0^1) = P(a_0 = 0)$, $P(s_0^2) = P(a_0 = 1)P(x_0^B = 0)$, and $P(s_0^3) = P(a_0 = 1)P(x_0^B = 1)$.

C. Merging gap constraints:

The longitudinal position between the two merging vehicles must be more than a threshold $d_r > 0$ for accident prevention during lane merging. This condition formulates the merging gap constraints:

$$|x_{k,1}^r - x_{k,1}^h| \geq d_r, \quad (14)$$

where $x_{k,1}$ denotes the position state. The detailed formulation can be found in [8].

D. Chance constraints

Any solutions that have a low chance of occurring are removed from the list of potential solutions using chance constraints. The potential human state transition events in our formulation are $T_k = [t_k^1\ \ldots\ t_k^{n^2}\ \bar{t}_k^1\ \ldots\ \bar{t}_k^{n^2}]^\top$ and the transition probabilities are $P = \left[P[t_k^1]\ \ldots\ P[t_k^{n^2}]\ P[\bar{t}_k^1]\ \ldots\ P[\bar{t}_k^{n^2}]\right]^\top$. The chance constraint becomes

$$\sum_{k=0}^{K-1} \sum_{i=1}^{n^2} \left(t_k^i \ln(P[t_k^i]) + \bar{t}_k^i \ln(P[\bar{t}_k^i]) \right) \geq \ln(\tilde{p}), \quad (15)$$

with $\tilde{p} \in [0, 1]$ being a probability bound. This chance constraint (15) enforces that T realizes with at least $\tilde{p}$ probability.

V. Stochastic MPC formulation

The sMPC aims to meet all the constraints necessary to model the coordination of the IHV and the AV while optimizing the decision variables at each time step k. All the aforementioned constraints are accumulated and formulated as inequality constraints $G_k \theta_k \leq g_k$, where $G_k \in \mathbb{R}^{n_c \times n_t}$, $g_k \in \mathbb{R}^{n_c \times 1}$, n_t is the total number of decision variables, and n_c is the total number of constraints. The decision variable set θ_k contains the future K steps of variables necessary to formulate the model and the inputs we want to optimize.

We optimize a cost function as a weighted sum of five objectives: minimizing control inputs, minimizing time for achieving the merging distance, maximizing AV and IHV speed, minimizing the number of advisory directives, and maximizing the probability of stochastic events. The combined cost function is given by

$$J(\theta_k) = \theta_k^\top Q \theta_k + c^\top \theta_k, \quad (16)$$

where $Q \in \mathbb{R}^{n_t \times n_t}$, $c \in \mathbb{R}^{1 \times n_t}$ are the designed objective weights for the system. The weights are important factors in determining optimal maneuvers of the vehicles. A human driver's long-term driving data may be compiled to assess how much weight to be assigned to each of the objectives. In the experiments, we manually tune the weights to produce desired vehicle behaviors.

To evaluate the effect of advisory commands on humans, we create two sMPC setups: 1) multi-advisory setup and 2) max-one advisory setup. For the multi-advisory setup, the system is allowed to advise multiple times to influence the human driver. The max-one advisory setup is allowed to advise once to influence the driver's behavior. To enforce this condition in the max-one advisory setup, we use an additional constraint on the number of advisory commands:

$$u_0^B + u_1^B + \cdots + u_K^B \leq 1. \quad (17)$$

Once an advisory command is issued, no advisory commands will be generated in the future.

Considering the current human state as a deterministic parameter, the sMPC optimization problem is formulated as

$$\min_{\theta_k}\ J(\theta_k), \quad s.t.\ \ \mathbf{G}_k \theta_k \leq \mathbf{g}_k. \quad (18)$$

However, the human state is an uncertain parameter that can only be estimated. To tackle this stochasticity of the human

state, we formulate three sets of optimization that correspond to three possible human states. If the human is in s^1, s^2, or s^3 state, the optimized decision variables are denoted by θ_k^1, θ_k^2 and θ_k^3 respectively. Based on the probabilities of each state, we solve the following sMPC

$$\min_{\theta_k^1,\theta_k^2,\theta_k^3} \quad J(\theta_k^1,\theta_k^2,\theta_k^3) = P(s_k^1)\left((\theta_k^1)^\top Q\theta_k^1 + c^\top\theta_k^1\right) + P(s_k^2)\left((\theta_k^2)^\top Q\theta_k^2 + c^\top\theta_k^2\right) + P(s_k^3)\left((\theta_k^3)^\top Q\theta_k^3 + c^\top\theta_k^3\right) \quad (19)$$

$$\text{s.t.} \quad P(s_k^1)\mathbf{G}_k\Big|_{s_k^1=1}\theta_k^1 \le P(s_k^1)\mathbf{g}_k\Big|_{s_k^1=1}, \quad (20)$$

$$P(s_k^2)\mathbf{G}_k\Big|_{s_k^2=1}\theta_k^2 \le P(s_k^2)\mathbf{g}_k\Big|_{s_k^2=1} \quad (21)$$

$$P(s_k^3)\mathbf{G}_k\Big|_{s_k^3=1}\theta_k^3 \le P(s_k^3)\mathbf{g}_k\Big|_{s_k^3=1} \quad (22)$$

$$[u_k^r\ u_k^a\ u_k^B]^\top\Big|_{s_k^1=1} = [u_k^r\ u_k^a\ u_k^B]^\top\Big|_{s_k^2=1} = [u_k^r\ u_k^a\ u_k^B]^\top\Big|_{s_k^3=1}. \quad (23)$$

The constraint (23) enforces that the control inputs to be implemented on the AV and the IHV must be the same for the three possible states. The sMPC solution provides the control inputs applied to the AV and the advisory commands conveyed to the IHV at each time step. After the inputs are implemented, the optimization moves one step forward with the new human state estimates and initial conditions and calculates the optimal input for the next time step.

VI. Simulation Results

In simulations, we apply the aforementioned sMPC formulation. For vehicle dynamics, a double integrator model is used. Up until the safe merging distance of $d_r = 7m$ is reached, the sMPC optimization is solved based on the vehicle states, human input prediction, and the human state probabilities to provide the input for the AV and the advisory command for the IHV. The look-ahead window is $K = 10$ for all simulations, and each time step is 0.8 seconds. We used the Gurobi solver [16] to solve the optimization problem.

In Fig. 3, an attentive driver (left column) is simulated to transition to following advisory after the advisory announcement. We observe that the merging action is distributed between the IHV and the AV and the attentive driver is advised to speed up where the AV slows down to perform the merging. An inattentive driver (right column) is simulated to stay distracted throughout the merge. For the inattentive driver, the system advises the driver to decelerate more in the initial two steps. As the human is distracted, the AV takes up more merging action in the initial two time steps with a higher acceleration compared to the attentive scenario. Toward the end, the system advises the human in both attentive and inattentive scenarios to keep a steady speed.

The simulation results show that the sMPC formulation generates coordinated merging trajectories for both vehicles We then implement the sMPC on a HITL experiment testbed to test its performance with a real human driver.

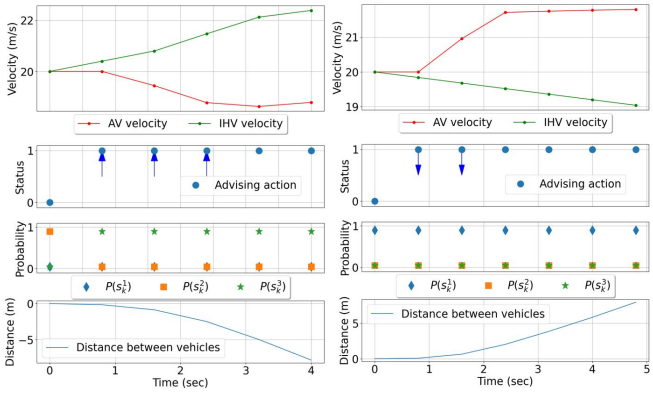

Fig. 3. Simulation results with multi-advisory setup for human attentive (left column) and human inattentive (right column). Upwards, downward arrows, and no arrow in advising action when the advising state is 1 indicate speed-up, slow-down, and keep speed advising respectively.

VII. Experimental Results

For HITL experimentation, we developed a driving simulator testbed, a detailed description of which can be found in [17]. Using this testbed, we conducted 30 merging tests with two advisory setups: 1) multi-advisory setup and 2) max-one advisory setup on a human driver volunteer with proficient driving experience. Half of the tests were completed with the driver being attentive, and the other half with the driver exhibiting one of the 7 distracted driving behaviors. Based on the optimization results, the AV input and the IHV advisory command are updated every 0.8 seconds. Given the advisory command, the copilot announces 'speed up', 'slow down', or 'keep' to advise the human to speed up, slow down or keep speed, respectively. The current speed and the advised speed derived from the advised acceleration are shown on a speed circular chart on a display screen.

In Fig. 4(a), the performance of the sMPC in the multi-advisory setup with an attentive driver (left column) and an inattentive driver (right column) is presented. The attentive driver tries to follow the advisory commands and increase the speed of the vehicle initially. After the third time step, the system advises the driver to keep speed since the distance for merging is about to be established. On the other hand, the inattentive driver slows down with a small deceleration and is advised to slow down more. In the last four steps, the human is advised to keep speed to prevent unnecessary slowdown. But as the driver is inattentive, she/he does not follow the commands and decelerates at her/his own rate.

Fig. 4(b) illustrates the performance of the sMPC in the max-one advisory setup for an attentive driver (left column) and an inattentive driver (right column). Initially, the attentive driver speeds up slightly, so the sMPC advises the IHV to accelerate while the AV slows down to facilitate the merge. The inattentive driver who also slightly speeds up in the beginning, is also advised to speed up more. But compared to the attentive scenario the inattentive driver accelerates less. Thus, the AV decelerates at a higher rate than in the attentive case to achieve the safe merging distance quickly.

Table II shows the average merging time for each scenario.

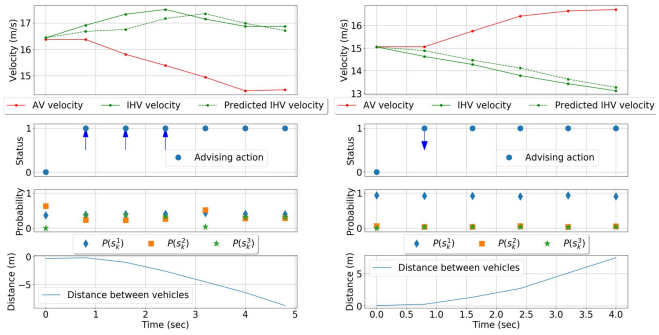

(a) Multi-advisory

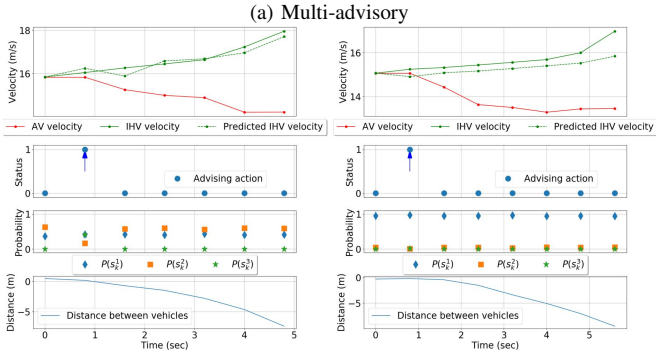

(b) Max-one advisory

Fig. 4. HITL driving experimental results for human attentive (left column) and human inattentive (right column). Upwards, downward arrows, and no arrow in advising actions when the advising state is 1 indicate speed-up, slow-down, and keep speed advising respectively.

TABLE II

AVERAGE TIME TO MERGE (SECONDS)

Scenario	Attentive	Inattentive
Multi-advisory	4.53	5.17
Max-one advisory	5.12	5.28

Comparing the time for the 30 tests, it is evident that the sMPC algorithm successfully generates effective merging scenarios for both attentive and inattentive human drivers. Comparing between the multi-advisory and max-one advisory, the average merging time is slightly higher for max-one advisory for both attentive and inattentive drivers. This is expected as the max-one advisory has a limited chance to advise the human and influence their action.

We conclude from these findings that the sMPC algorithm provides appropriate merging solutions for both attentive and inattentive drivers with a reasonable merging time. Moreover, the advisory commands play a vital role in the coordination of the AV and IHV. With less advisory commands in the max-one advisory setup, there is less control over the human driver thus the time for the merge are comparatively higher than the multi-advisory setup.

VIII. CONCLUSIONS AND FUTURE WORK

We present an sMPC formulation that takes human states into consideration to coordinate the motion of an IHV and an AV for optimal merging. The formulation includes state variables affecting a human driver's behavior, such as attention and tendency to follow advisory commands. The sMPC solution takes the stochasticity of human behaviors into account and produces optimal inputs for the AV and advisory instructions for the IHV. By conducting simulations and experiments, we demonstrate the effectiveness of the proposed approach. In the future, we plan to improve the model of human driver behaviors by incorporating additional human states, such as aggressively driving and conservatively driving and studying their responses in challenging driving conditions, such as in a platoon.

REFERENCES

[1] "Autonomous Vehicle Sales Forecast 2018 - AutoTechInsight," [Online; accessed 2022-11-23]. [Online]. Available: https://autotechinsight.ihsmarkit.com/shop/product/5001816/autonomous-vehicle-sales-forecast-2018

[2] C.-P. Lam, A. Y. Yang, K. Driggs-Campbell, R. Bajcsy, and S. S. Sastry, "Improving human-in-the-loop decision making in multi-mode driver assistance systems using hidden mode stochastic hybrid systems," in *2015 IEEE/RSJ International Conference on Intelligent Robots and Systems (IROS)*, 2015, pp. 5776–5783.

[3] C.-P. Lam and S. S. Sastry, "A POMDP framework for human-in-the-loop system," in *53rd IEEE Conference on Decision and Control*, 2014, pp. 6031–6036.

[4] X. Huang, A. Jasour, M. Deyo, A. Hofmann, and B. C. Williams, "Hybrid risk-aware conditional planning with applications in autonomous vehicles," in *2018 IEEE Conference on Decision and Control (CDC)*. IEEE, 2018, pp. 3608–3614.

[5] C. Hubmann, M. Becker, D. Althoff, D. Lenz, and C. Stiller, "Decision making for autonomous driving considering interaction and uncertain prediction of surrounding vehicles," in *2017 IEEE Intelligent Vehicles Symposium (IV)*. IEEE, 2017, pp. 1671–1678.

[6] S. Mosharafian and J. M. Velni, "Cooperative adaptive cruise control in a mixed-autonomy traffic system: A hybrid stochastic predictive approach incorporating lane change," *IEEE Transactions on Vehicular Technology*, pp. 1–13, 2022.

[7] D. A. Lazar, R. Pedarsani, K. Chandrasekher, and D. Sadigh, "Maximizing road capacity using cars that influence people," in *2018 IEEE Conference on Decision and Control (CDC)*. IEEE, 2018, pp. 1801–1808.

[8] S. Hossain, J. Lu, H. Bai, and W. Sheng, "Stochastic model predictive control for coordination of autonomous and human-driven vehicles," *IFAC-PapersOnLine*, vol. 55, no. 41, pp. 142–147, 2022.

[9] ——, "Cooperative driving between autonomous vehicles and human-driven vehicles considering stochastic human input and system delay," in *2023 European Control Conference (ECC)*, 2023, pp. 1–6.

[10] J. Lu, S. Hossain, W. Sheng, and H. Bai, "Cooperative driving in mixed traffic of manned and unmanned vehicles based on human driving behavior understanding," in *2023 IEEE International Conference on Robotics and Automation (ICRA)*, 2023, pp. 3532–3538.

[11] S. Hossain, J. Lu, H. Bai, and W. Sheng, "Supplementary materials: Incorporating stochastic human driving states in cooperative driving between human-driven vehicle and autonomous vehicle," 2023. [Online]. Available: https://coral-osu.github.io/assets/pdf/IROS2023_Supplementary_Materials.pdf

[12] A. Bemporad and S. Di Cairano, "Model-predictive control of discrete hybrid stochastic automata," *IEEE Transactions on Automatic Control*, vol. 56, no. 6, pp. 1307–1321, 2010.

[13] C. C. Macadam, "Understanding and modeling the human driver," *Vehicle system dynamics*, vol. 40, no. 1-3, pp. 101–134, 2003.

[14] W. Hoult and D. J. Cole, "A neuromuscular model featuring co-activation for use in driver simulation," *Vehicle System Dynamics*, vol. 46, no. S1, pp. 175–189, 2008.

[15] A. Bemporad and M. Morari, "Control of systems integrating logic, dynamics, and constraints," *IEEE Transactions on Automatic Control*, vol. 35, pp. 407–427, 1999.

[16] Gurobi Optimization, LLC, "Gurobi Optimizer Reference Manual," 2022. [Online]. Available: https://www.gurobi.com

[17] J. Lu, R. Stracener, W. Sheng, H. Bai, and S. Hossain, "Development of a research testbed for cooperative driving in mixed traffic of human-driven and autonomous vehicles," in *2022 IEEE/RSJ International Conference on Intelligent Robots and Systems (IROS)*, 2022, pp. 11 403–11 408.